Constraint parameters along a three-dimensional crack front stress field

Yu.G. Matvienko

Mechanical Engineering Research Institute of the Russian Academy of Sciences
4 Kharitonievsky Per., 101990, Moscow, Russia
matvienko7@yahoo.com

V.N. Shlyannikov, N.V. Boychenko

Research Center for Power Engineering Problems of the Russian Academy of Sciences
Lobachevsky Street, 2/31, post-box 190, 420111, Kazan, Russia

ABSTRACT. In-plane and out-of-plane constraint effect on crack-front stress fields under creep conditions are studied by means of three-dimensional numerical analyses of finite thickness boundary layer models and different specimen geometries. This investigation is an extension of the modified boundary layer solution developed by Shlyannikov et al. in 2011 with special attention on constraint parameters of the nonlinear crack-tip fields for a solid of finite thickness. Characterization of constraint effects is given by using the non-singular T-stress, the local triaxiality parameter, the -factor of the stress-state in 3D cracked body and the second order term amplitude factor. The constraint parameters are determined for a center cracked plate, three-point bend specimen and compact tension specimen. Discrepancies in constraint parameters distribution along crack front towards thickness of the specimens have been observed under different loading conditions of creeping power law hardening material for various configurations of specimens.

KEYWORDS. In-plane and out-of-plane constraint parameters; Creep; Experimental specimens.

INTRODUCTION

Constraint effects in the vicinity of the crack tip have been extensively studied for a long time. However, all approaches can successfully describe the in-plane constraint effects, but they are limited to a planar case. The description of out-of-plane constraint should include specimen's dimension such as thickness. Only a few researches are carried out to describe thickness effect on crack-tip constraint (e.g., [1, 2]). Some authors [3, 4] showed that 3D crack-front constraint effect in a thin plate and in thick SENB specimens are well represented by $J - A_2$ three-term solution under small scale yielding and large scale yielding conditions.

Constraint effects in modern fracture mechanics are usually associated with specimen configuration and loading conditions and its effect on the crack-tip fields and the fracture toughness. Therefore, dependence of the fracture toughness is referred to these constraint parameters. In this case, the fracture toughness versus constraint parameters can be considered like the material failure curve or constraint master curve [5]. However, the general analysis of constraint effects requires to be defined more exactly in 3D problem taking into account in-plane and out-of plane constraint.

The present study focuses on the finite element analysis of the creeping material under different in-plane and out-of-plane constraint levels. The geometries considered in detailed three-dimensional finite element calculations are a finite thickness large circular domain containing a crack and most popular specimens in experimental fracture mechanics. The application of triaxiality parameter h, T_z–factor and the second order term amplitude A_2 to 3D crack-front stress field and the characterization of the interaction of in-plane and out-of-plane constraint have been discussed.

DETERMINATION OF CONSTRAINT PARAMETERS

I t is well known that different traditional approaches based on the T-stress or Q-parameter, which successfully describe in-plane constraint, are not accurate for 3D cracks. Thus, it is necessary to employ others parameters for describing the out-of-plane constraint. The T_z-factor introduced by Guo [2] allows estimating the constraint effect and the stress-state in a 3D cracked body:

$$T_z = \frac{\sigma_{zz}}{\nu\left(\sigma_{xx} + \sigma_{yy}\right)} \tag{1}$$

where ν is the Poisson's ratio, and $\sigma_{xx}, \sigma_{yy}, \sigma_{zz}$ are the stress tensor components.

Because the validity of the above-mentioned concepts depends on the chosen reference field, a local parameter of crack tip constraint and stress triaxiality was proposed by Henry and Luxmoore [6] as a secondary fracture parameter:

$$h(r,\theta,z) = \sigma_{kk}\bigg/\left(3\sqrt{\frac{3}{2}s_{ij}s_{ij}}\right) \tag{2}$$

where σ_{kk} and s_{ij} are hydrostatic and deviatoric stresses, respectively. Being such a parameter as a function of both first invariant of the stress tensor and the second invariant of the stress deviator, it is a local measure of in-plane and out-of-plane constraint that is independent on any reference field. The different combinations of load biaxiality and nominal stress level are characterized by the in-plane elastic nonsingular term [7]:

$$\sigma_{ij} = \frac{K}{\sqrt{2\pi r}} f_{ij}(\theta) + T\delta_{1i}\delta_{1j} \tag{3}$$

where K is the elastic stress intensity factor, r and θ are the polar coordinates and $f_{ij}(\theta)$ is the dimensionless angular stress function. The second term in the stress expansion is denoted as the T-stress and can be regarded as a stress parallel to the crack plane [8]. In this case, the magnitude of the T-stress is defined through elastic-plastic stress components for $\theta = 0°$:

$$T_{appl} = T/\sigma_y = \left(\left(\sigma_{xx} - \sigma_{yy}\right)/\sigma_y\right) \tag{4}$$

Yang et.al. [9] and Nikishkov [10] performed a complete analysis of three-term asymptotic fields for mode I plane strain conditions. They have shown that the first three terms of the asymptotic expansion are sufficient to represent the stress field in the crack tip vicinity for a power-law hardening material. It is assumed that the stress components near a crack tip can be expressed as a series:

$$\bar{\sigma}_{ij} = A_1 \bar{r}^{s1} \tilde{\sigma}_{ij}^{(1)}(\theta) + A_2 \bar{r}^{s2} \tilde{\sigma}_{ij}^{(2)}(\theta) + A_3 \bar{r}^{s3} \tilde{\sigma}_{ij}^{(3)}(\theta) + .. \tag{5}$$

where r and θ are polar coordinates centered at the crack tip, $\tilde{\sigma}_{ij}^{(k)}(\theta)$ are dimensionless angular functions and indexs 1,2,3 correspond to the first-order, second-order and third-order fields, respectively. A_1, A_2, A_3 are amplitude factors, and

s_1, s_2, s_3 are the exponents of stress functions. In the case of the creeping material, the first term amplitude factor A_1 can be obtained by replacing appropriate parameters. Using the Hoff analogy to contrast the power-law creep relation with the power-law hardening relation, Ridel and Rice [11] presented the HRR-type singularity field for power-law creep materials with amplitude A_1:

$$A_1(t) = \left(\frac{C(t)}{\dot{\varepsilon}_0 \sigma_0 I_n} \right)^{1/(n+1)} \tag{6}$$

where σ_0 is a reference stress, $\dot{\varepsilon}_0$ is a reference creep strain rate and n is the creep exponent. The amplitude factor $C(t)$ depends upon the applied time, the magnitude of the remote loading, the crack configuration and the material properties. According to solution (5), the amplitude of the second-order and third-order fields are not independent of each other and has a simple relationship:

$$A_3 = A_2^2 \tag{7}$$

The amplitude factor A_2 cannot be determined in the asymptotic analysis. Therefore, the values of A_2 are herein determined by matching the three-term stress solutions in Eq.(5) with known crack-tip fields, such as finite element results.
A dimensionless radial coordinate is given by:

$$\bar{r} = (\sigma_0 \dot{\varepsilon}_0 r / C) = (r/a) / \left(\pi \sqrt{n} \left(\frac{\sqrt{3}}{2} \frac{\sigma}{\sigma_0} \right)^{n+1} \right) \tag{8}$$

It should be noted that for creeping material the amplitude factors in the three-term solution (Eq.(5)) generally depend on the creep time, magnitude of the applied loading, crack geometry and material properties. Due to the complexities, different creeping stages are considered in the present work. It is useful to normalize a current creep time t by the characteristic time t_T for transition from small-scale creep to extensive creep:

$$\frac{t}{t_T} = \frac{t(n+1)EC}{(1-v^2)K_I^2} \tag{9}$$

where K_I is the elastic stress intensity factor, v is the Poisson's ratio, E is the Young's modulus.
The ANSYS [12] finite element code is used to solve modified boundary layer problem and to analyze stress-strain state of specimens. The FEA calculations are based on the J_2 incremental theory of plasticity. A similar coordinate system is employed. The x-axis lies in the crack plane and is normal to the straight crack front; y-axis is orthogonal to the crack plane and z-axis lies on the thickness direction. The origin of the coordinate system is located at the crack tip on the center plane. Along the thickness direction, the identical planar mesh is repeated from the symmetry plane (z/b=0.5) to the free surface (z/b=0). In order to catch the drastic change of the stress field near the free surface, thickness of successive element layers is exponentially reduced from the mid-plane toward the free surface. In the circumferential direction, 40 equally sized elements are defined in the angular region from 0 to π. The size of each ring gradually increases with the radial distance from the crack tip. Radial sizes of elements are varied according to the geometric progression.
For a pure power-law creeping material behavior governed by the Norton constitutive relation under uniaxial tension, the total strain rate is related to the stress by the following relationship:

$$\dot{\varepsilon} = \dot{\varepsilon}_0 \left[\frac{\sigma}{\sigma_0} \right]^n \text{ or } \dot{\varepsilon} = \bar{B}\sigma^n \tag{10}$$

The material constants E, v, σ_y, m, n, σ_0, $\dot{\varepsilon}_0$ or $\bar{B}$ are obtained experimentally from uniaxial tests at the certain temperature. For the present problem, Young's modulus, Poisson's ratio and yield stress are considered to be equal to 205

GPa, 0.3 and 380 MPa, respectively. The strain hardening exponent *m* is 4.96. The creep parameter and the creep exponent are $\bar{B}=1.4\cdot 10^{-10}$ and *n*=3. The reference stress and reference creep strain rate are $\sigma_0=100$MPa and $\dot{\varepsilon}_0=1.1\cdot 10^{-7}$ hour^{-1}.

RESULTS AND DISCUSSION

F ull-field 3D finite element analyses are carried out to determine the elastic-plastic and creep stress fields along the through-thickness crack front in a circular disk and experimental specimens subjected to different type loadings. The following problem and typical specimen configurations are considered (Fig.1):
(a) – modified boundary layer problem with displacement boundary conditions (MBLP);
(b) – center cracked tension (CCT) specimen;
(c) – single edge notched bend (SENB) specimen;
(d) – compact tension (CT) specimen.
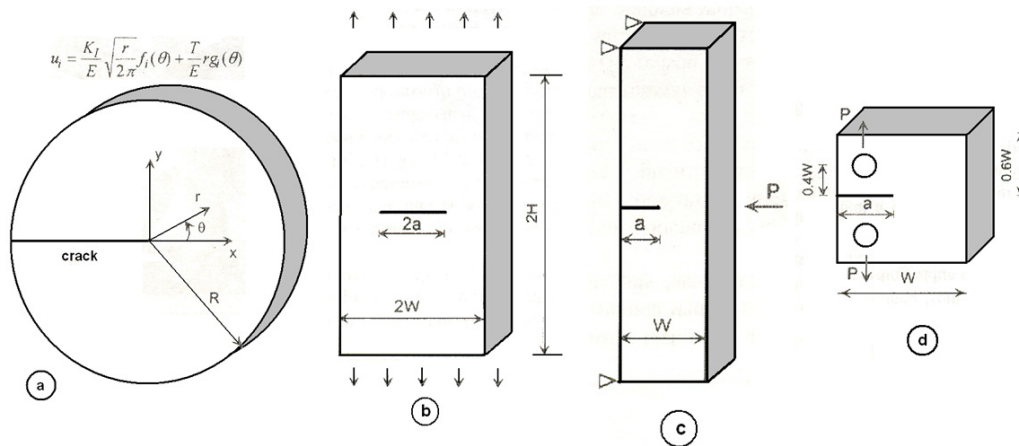
Figure 1: (a) – modified boundary layer problem and specimens, (b) – CCT specimen; (c) – SENB specimen; (d) – CT specimen.

First of all, the T-stress distribution ahead of the crack-tip (θ=0°) under mode I was investigated. The distribution of the in-plane constraint parameter along the crack front in the thickness direction is plotted in Fig. 2 for different specimen geometries. The effect of the creep time on the computed dimensionless values of the T-stress, which are normalized by the applied nominal stress for a cracked bodies (the crack aspect ratio a/W=0.5), has been analyzed. It can be seen from Fig. 2 that the T-stress decreases significantly with the increase of creep time for all specimens. It means that the in-plane constraint is lost when nonlinear stress-strain state changes from the small-scale creep conditions to the extensive creep conditions. As follows from Fig. 2, the SENB specimen is more constrained by the in-plane parameter with respect to other geometries of the specimens. It can be also seen that the in-plane constraint parameter decreases along the crack front toward the specimen free surface.
The distribution of the out-of-plane constraint parameters along the crack front in the thickness direction is plotted in Fig. 3 for different specimens and modified boundary layer problem. The left row in Fig. 3 depicts the behavior of the T_z-factor, while the right row in Fig. 3 gives distribution of the stress triaxiality parameter h under pure mode I loading. The constraint parameters are plotted against the normalized specimen thickness z/b. It can be seen from these figures that the out-of-plane constraint parameters decrease along the crack front toward the free surface. In contrast to the T_z-factor and the triaxiality parameter h distributions at the center plane (z/b=0.5), FEA results show great relaxation of the crack-front constraint at the plane near the free surface (z/b=0.0125). At the same time, the out-of-plane constraint parameters T_z and h increase slightly through most part of the thickness toward the mid-plane.
Through-thickness variations of the first order term amplitude A_1 and the second order term amplitude A_2 at the crack front for creeping material in the case of different cracked specimen geometries and loading conditions are shown in Fig. 4. These distributions relate to wide range of dimensionless creep time from the small scale creep conditions, characterized by $\bar{t}=0.0925$, to extensive creep conditions $\bar{t}=46.25$ when the radial distance r is normalized by

$C/(\sigma_0\dot{\varepsilon}_0)$. For creeping material both the first order term amplitude A_1 and the second order term amplitude A_2 are the out-of-plane constraint parameters which are more sensitive to the in-plane constraint and different specimen configuration.

Generally, it can be concluded that the second order term amplitude A_2 efficiently represents the out-of-plane constraint effect on the nonlinear creep crack-front stress fields for different specimens throughout thickness. The present results are addressed to constraint loss in the full three-dimensional problem which combines constraint loss effects due to in-plane effects and out-of-plane effects for the specimens of different geometry.
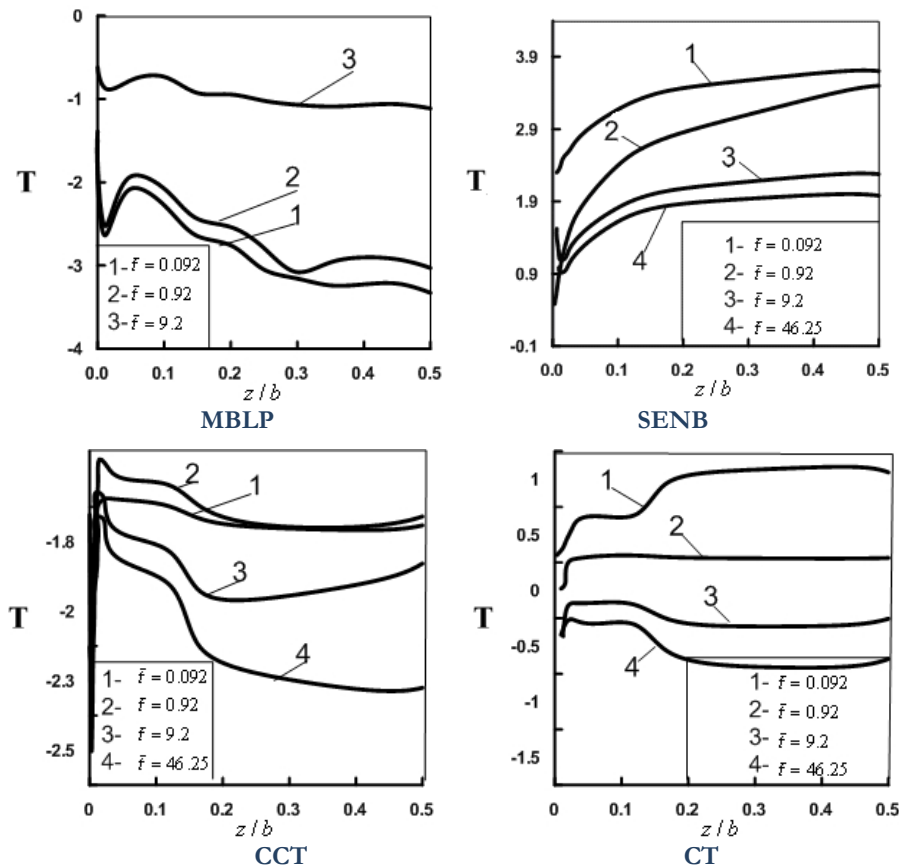
Figure 2: The T-stress distribution through thickness for different cracked geometries.

CONCLUSIONS

In-plane and out-of-plane constraint parameters are studied numerically taking into account the interaction between loading conditions, specimen geometries and cracked body thickness. The following constraint parameters have been employed, namely, the T_z-factor, the stress triaxiality parameter h, the non-singular T-stress, the first A_1 and the second A_2 terms in the 3D series of creep crack tip stress fields. Discrepancies in distribution of the constraint parameters along crack front towards thickness of the cracked body have been observed under different loading conditions of creeping power law hardening material for various configurations of the specimens. It is found that the out-of-plane constraint parameter behavior strongly depends on the creep time. Numerical results indicate that there is a distinct relationship between the in-plane and out-of-plane crack-front constraint, which can be described by non-singular term in the series of crack tip stress fields. The relationship between 3D crack front constraint parameters in terms of T and A_2, T_z, h and thickness of the specimens can be drawn and with it the combined effect of in-plane and out-of-plane constraint on the fracture toughness should be analyzed.
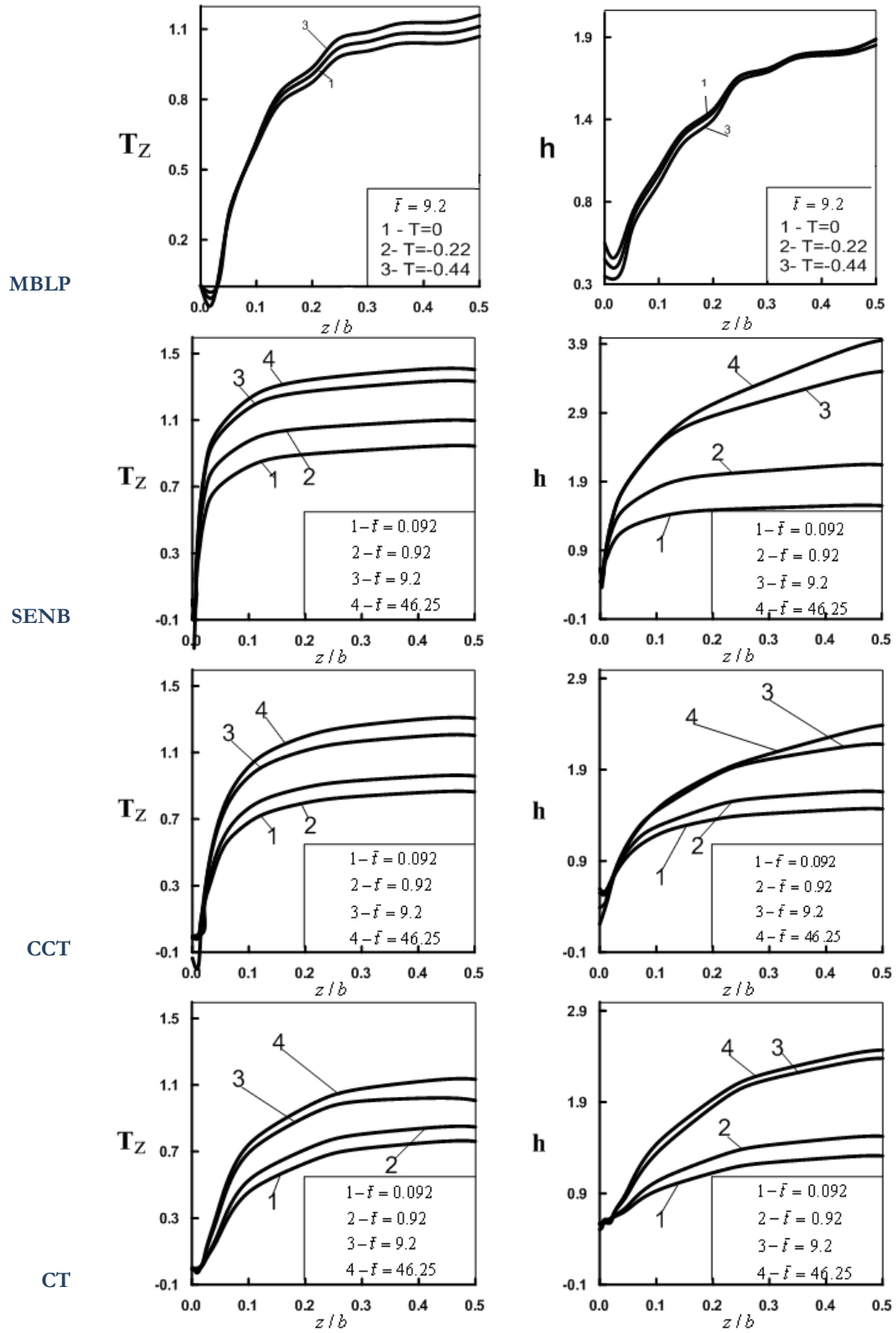
Figure 3: Variation of constraint parameters through thickness for different cracked geometries.

Figure 4: Variation of amplitude factors through thickness for different cracked geometries.
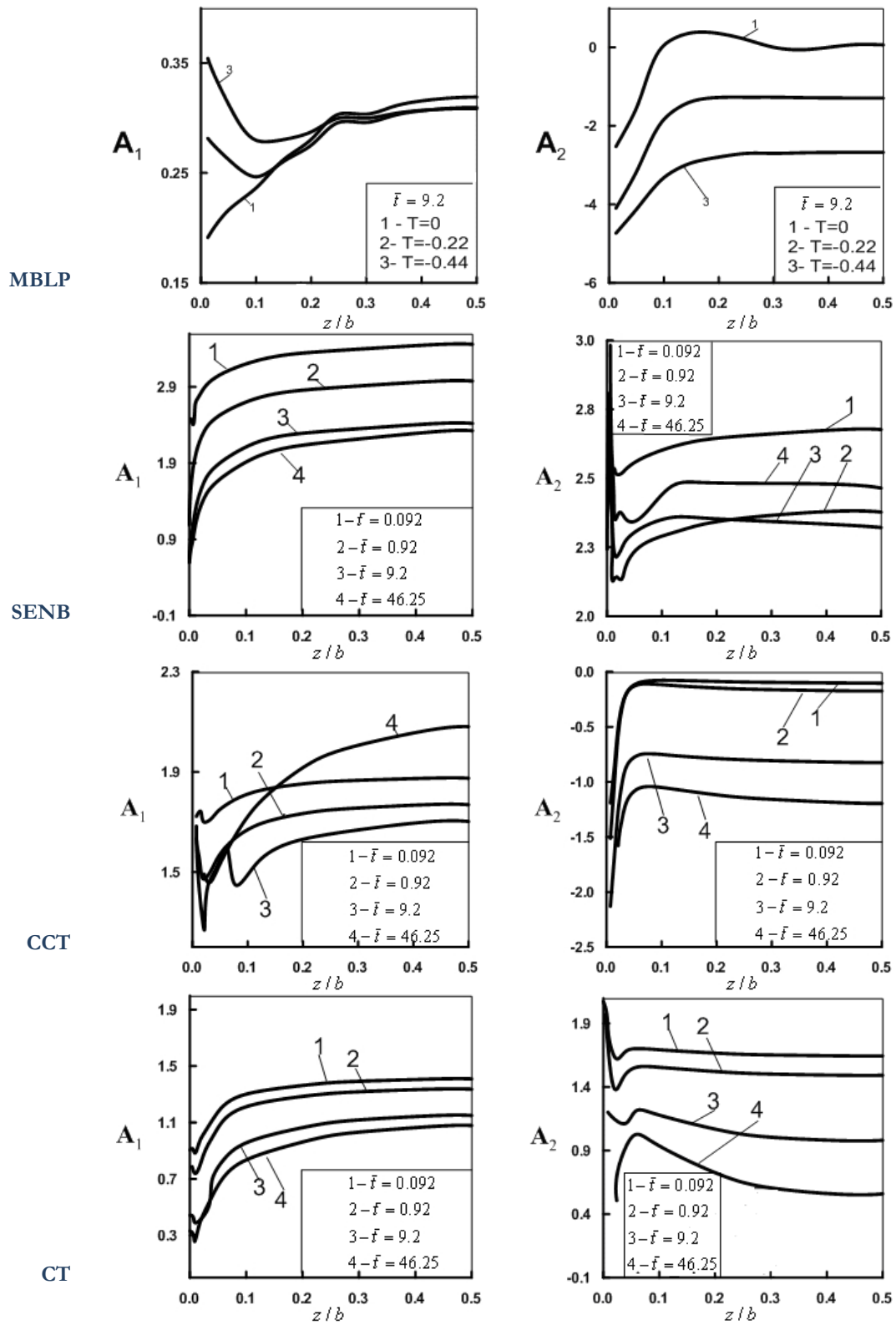
REFERENCES

[1] V. N. Shlyannikov, N. V. Boychenko, A. M. Tartygasheva, Engng. Fract. Mech., 2011 (article in press).
[2] W. L. Guo., Engng. Fract. Mech., 46 (1993) 93.
[3] Y. Kim, Y. J. Cha, X. K. Zhu, Int. J. Solid. Struct., 40 (2003) 6267.
[4] Y. Kim, X. K. Zhu, Y. J. Cha, Engng. Fract. Mech, 68 (2001) 895.
[5] H. M. Meliani, Yu. G. Matvienko, G. Pluvinage, Int. Journal Fract., 167 (2011) 173.
[6] B. S. Henry, A. R. Luxmoore, Engng. Fract. Mech., 57 (1997) 375.
[7] J. Eftis, N. Subramonian, Engng. Fract. Mech., 10 (1978) 43.
[8] J. R. Rice, J. Mech. Phys. Solids., 22 (1974) 17.
[9] S. Yang, Y. J. Chao, N. A. Sutton, Engng. Fract. Mech., 45 (1993) 1.
[10] G. P. Nikishkov, Engng. Fract. Mech., 50 (1995) 65.
[11] H. Riedel, J. R. Rice, ASTM STP 700 (1980) 112.
[12] ANSYS Structural Analysis Guide. 001245. Fifth Edition. SAS IP, Inc (1999).